Parent Hamiltonian reconstruction via inverse quantum annealing

Davide Rattacaso, ^{1, 2, a} Gianluca Passarelli, ³ Angelo Russomanno, ⁴ Procolo Lucignano, ¹ Giuseppe E. Santoro, ^{5, 6, 7} and Rosario Fazio ^{6, 1}

Dipartimento di Fisica "E. Pancini", Università di Napoli "Federico II", Monte S. Angelo, I-80126 Napoli, Italy Dipartimento di Fisica e Astronomia "G. Galilei", Università di Padova, I-35131 Padova, Italy 3 CNR-SPIN, c/o Complesso di Monte S. Angelo, via Cinthia - 80126 - Napoli, Italy 4 Scuola Superiore Meridionale, Università di Napoli Federico II, Largo San Marcellino 10, I-80138 Napoli, Italy 5 SISSA, Via Bonomea 265, I-34136 Trieste, Italy 6 The Abdus Salam International Center for Theoretical Physics, Strada Costiera 11, 34151 Trieste, Italy 7 CNR-IOM Democritos National Simulation Center, Via Bonomea 265, I-34136 Trieste, Italy (Dated: March 23, 2023)

Finding a local Hamiltonian having a given many-body wavefunction as its ground state is a serious challenge of fundamental importance in quantum technologies. Here we introduce a method, inspired by quantum annealing, that efficiently performs this task through an artificial inverse dynamics: a slow deformation of the state generates an adiabatic evolution of the corresponding Hamiltonian. We name this approach *inverse quantum annealing*. This method only requires the knowledge of local expectation values. As an example, we apply inverse quantum annealing to find the local Hamiltonian of fermionic Gaussian states.

Introduction.— The success of quantum technologies ultimately relies on our ability to control increasingly complex artificial quantum systems [1]. This may require, in quantum simulators, the accurate tailoring of a many-body Hamiltonian. For this reason, controlling [2, 3] and verifying [4, 5] the actual functioning of these systems have raised increasing attention to the search for parent Hamiltonians (PHs) [6– 14]. This problem consists in finding a realistic Hamiltonian, i. e., local and/or engineerable, having a given wavefunction as a ground state. The knowledge of a parent Hamiltonian is related to Hamiltonian learning [15–17] and verification of quantum devices, and can be exploited to experimentally prepare a target ground state. The search for a parent Hamiltonian represents an especially complex instance of the reconstruction of a Hamiltonian from one of its eigenstates [18-22] or time-dependent states [23–26]. In particular, the space of the Hamiltonians having a given state as an eigenstate can be efficiently reconstructed from correlation functions [14, 18, 19] or expectation values of local commutators [20]. Picking PHs in this space is a hard task since it generally requires the diagonalization of all the candidate PHs to verify that the target state is a ground state [14]. More efficient methods have been suggested to obtain approximate PHs. These are based on the minimization of some cost functional of the partition function that can be very hard to evaluate [21, 22].

In this manuscript, we propose a new route to determine the parent Hamiltonian of a given many-body state. We introduce an *inverse quantum annealing* (IQA) method. It is inspired by quantum annealing [27–31], but swapping the role of quantum states and Hamiltonians (see Fig. 1). Initializing the system with a simple many-body state with a known PH, the procedure consists in slowly deforming the state towards the target state. The PH correspondingly evolves according to an artificial dynamics that becomes adiabatic if the deformation is slow enough. In the following, we will introduce the idea defining the IQA and we provide a concrete, exactly solvable example to test the method, highlighting the determination of

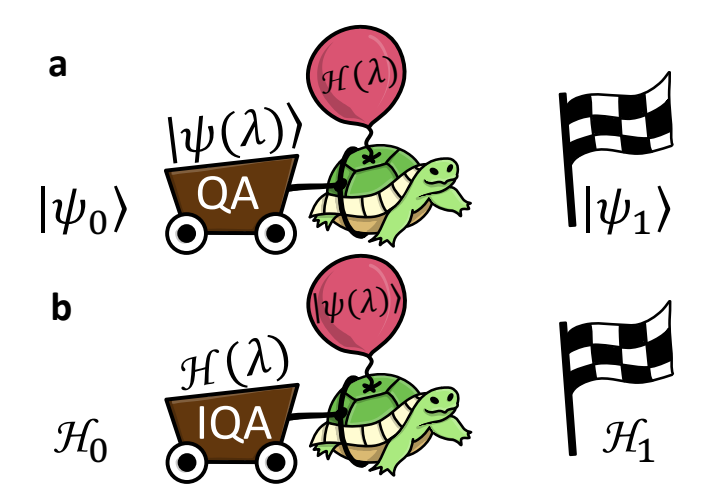


FIG. 1. (a): In the typical scheme of quantum annealing, the parametric Hamiltonian $\mathcal{H}(\lambda)$ interpolates between \mathcal{H}_0 , whose ground state $|\psi_0\rangle$ is known, and \mathcal{H}_1 , whose ground state $|\psi_1\rangle$ needs to be determined. A unitary evolution generated by $\mathcal{H}(\lambda)$ (the tortoise) is able to slowly carry $|\psi(\lambda)\rangle$ from $|\psi_0\rangle$ to $|\psi_1\rangle$ in the adiabatic limit $\dot{\lambda}(t)=0$. (b): In inverse quantum annealing, we introduce a family of states $|\psi(\lambda)\rangle$ connecting $|\psi_0\rangle$, whose parent Hamiltonian \mathcal{H}_0 is known, to $|\psi_1\rangle$, whose parent Hamiltonian needs to be determined. The IQA dynamics (the tortoise) is defined in such a way that, starting from \mathcal{H}_0 , the algorithm will slowly carry $\mathcal{H}(\lambda)$ to the desired \mathcal{H}_1 in the adiabatic limit.

the parent Hamiltonian and the IQA protocol.

Inverse quantum annealing protocol.— The determination of the parent Hamiltonian can be stated as follows. Given a (many-body) state $|\psi\rangle$, the task is to find a (local) Hamiltonian $\mathcal H$ for which $|\psi\rangle$ is the ground state. To this aim, we introduce a method inspired by the search of ground states employing adiabatic evolution [31]. The first step is to introduce a family of states $|\psi(\lambda)\rangle$ depending on a parameter $0 \le \lambda \le 1$ such that: i) $|\psi(1)\rangle \equiv |\psi_1\rangle$ is the quantum state for which a PH $\mathcal H_1$ needs to be determined, and ii) $|\psi(0)\rangle \equiv |\psi_0\rangle$ is a simple initial

state for which the PH \mathcal{H}_0 is easily known. For example, $|\psi_0\rangle$ can be the ground state of noninteracting spins in an external magnetic field. As shown in Fig. 1, in analogy with quantum annealing, we seek a dynamics that, by changing $\lambda(t)$ with time, in the adiabatic limit $\dot{\lambda}(t) \to 0$, guarantees that starting from \mathcal{H}_0 leads to the desired \mathcal{H}_1 . Any dynamics that satisfies these requests is suitable for IQA.

We choose an evolution dictated by

$$\partial_t \mathcal{H} = -i[\Pi(\lambda(t)), \mathcal{H}], \qquad (1)$$

where $\Pi(\lambda) = J|\psi(\lambda)\rangle\langle\psi(\lambda)|$ and J is an arbitrary energy scale.

Despite the apparent analogy with the Liouville equation for a density matrix, the evolution defined in Eq. (1) is artificial, not corresponding to any physical law. Eq. (1) will be the starting point for IQA. The evolution described by this equation is unitary, therefore $\mathcal{H}(t)$ is isospectral to $\mathcal{H}(0) \equiv \mathcal{H}_0$. We introduce $|\phi_{\alpha}(\lambda)\rangle$ as the instantaneous eigenstates of $\mathcal{H}(t)$, where α is a discrete index and $\alpha = 0$ labels the nondegenerate ground state $|\phi_0(\lambda)\rangle$, which at t = 0 corresponds to $|\psi_0\rangle$. The time-dependent $\mathcal{H}(t)$, solution of Eq. (1) is given by

$$\mathcal{H}(t) = \sum_{\alpha} E_{\alpha} U_{\pi}(t) |\phi_{\alpha}(t)\rangle \langle \phi_{\alpha}(t)| U_{\pi}^{\dagger}(t)$$
 (2)

where, in the adiabatic limit, the evolution operator U_{π} ensures $\mathcal{H}(t)$ to be the instantaneous PH, i. e.,

$$U_{\pi}(t)|\phi_0(\lambda)\rangle = \mathcal{T}(e^{-i\int_0^t dt'\Pi(t')})|\psi(0)\rangle \approx e^{i\omega(t)}|\psi(t)\rangle.$$
(3)

The adiabatic regime leading to the approximate evolution in the r. h. s. of Eq. (3) is guaranteed by the gap J in the spectrum of the operator $\Pi(\lambda)$. In the adiabatic limit, Eq. (1) generates PHs for states, thus performing an IQA protocol. This is guaranteed independently of the specific path of states defined by $\lambda(t)$ (as long as adiabaticity is preserved). The reason relies on the fact that $|\psi(\lambda)\rangle$ is a nondegenerate eigenstate $\Pi(\lambda)$. The rest of the spectrum of $\Pi(\lambda)$ is degenerate, and therefore the eigenstates $|\phi_{\alpha}(\lambda)\rangle$ with $\alpha \neq 0$ depend on the adiabatic path chosen [32].

An essential property to impose on \mathcal{H} is locality. The space of *l*-local Hamiltonians is formed by linear combinations of a set $\mathcal{L}^{(l)} = \{L_i^{(l)}\}\$ of interactions with maximum range l. As an example, a 2-local Hamiltonian is the 1D Ising Hamiltonian $H^{\text{Ising}} = \sum_{i} \sigma_{i}^{x} \sigma_{i+1}^{x}$, where σ_{i}^{x} is the x Pauli matrix acting on the *i*-th site of the chain. Any *l*-local Hamiltonian is written as $\mathcal{H} = \sum_{i} h_{i} L_{i}^{(l)}$ and is therefore identified by the couplings h_i . In general, we call local a Hamiltonian whose interaction range l does not depend on the system size N. Since $|\psi(\lambda)\rangle$ is a ground state of $\mathcal{H}(\lambda)$, we expect that $\mathcal{H}(\lambda)$ is a local Hamiltonian when $|\psi(\lambda)\rangle$ has finite correlation length. Even if the IQA is not directly affected by the closure of the first energy gap in the PH (see Eq. (3)), a diverging correlation length in some states of the path $|\psi(\lambda)\rangle$ may represent an obstacle in its realization. Notably, these two different conditions are both associated with a path of states, or Hamiltonians, crossing a quantum phase transition.

We use a time-dependent variational principle (TDVP) [33] to find an optimal l-local parent Hamiltonian as the adiabatic solution of Eq. (1). Indeed the TDVP allows determining the Hamiltonian couplings $h_i(t)$, by projecting the right hand side of Eq. (1) on the space $\mathcal{L}^{(l)} = \{L_i^{(l)}\}$ through the Hilbert-Schmidt distance $d(A,B) = \sqrt{\text{Tr}(A-B)^2}$, a natural Euclidean structure in the space of Hermitian operators. Hence we write the resulting evolution as

$$\partial_t \mathcal{H} = \mathbb{P}_l \left(-i \left[\Pi(\lambda(t)), \mathcal{H} \right] \right) , \tag{4}$$

where the projector $\mathbb{P}_l(A)$ defines the closest *l*-local operator *B* to the given operator *A*:

$$\mathbb{P}_{l}(A) = \operatorname{Argmin}_{B = \sum_{i} h_{i} L_{i}^{(l)}} \operatorname{Tr}(B - A)^{2} . \tag{5}$$

This approach, whose details are given in Supplemental Material [34], leads to the following equation for the coefficients $h_i(t)$ of the l-local Hamiltonian:

$$\partial_t h_i(t) = \sum_j K_{ij}^{(l)} \left[\psi(\lambda(t)) \right] h_j(t) , \qquad (6)$$

where

$$K_{ij}^{(l)}\left[\psi(\lambda)\right] \equiv i \langle \psi(\lambda) | \left[L_i^{(l)}, L_j^{(l)}\right] | \psi(\lambda) \rangle \tag{7}$$

is a skew-symmetric matrix that we name *commutator matrix*. Equation (6) is the central result of this work. In the adiabatic regime, it allows us determining the optimal l-local Hamiltonian starting from the given one. The accuracy of the method depends on the properties of the matrix $K_{ij}^{(l)}$. The entries of this matrix are the expectation values of local observables, showing non-analyticities only at phase transitions. When $|\psi(\lambda)\rangle$ has a finite correlation, these entries become independent of the system size for large N and the method rapidly converges. The kernel of the commutator matrix has been used in previous works to reconstruct local Hamiltonians from their eigenstates [20]. Previous methods however could not guarantee to find Hamiltonians having $\psi(\lambda)$ as the ground state. The IQA, when implemented through Eq. (6), can select the PH in this kernel without explicit diagonalization.

To verify when the adiabatic evolution is achieved, we will calculate the relative Hilbert-Schmidt operator distance

$$R_{T,\Delta T}(\lambda) = \sqrt{\operatorname{Tr}\left[\left(\mathcal{H}_{T+\Delta T}(\lambda) - \mathcal{H}_{T}(\lambda)\right)^{2}\right]/\operatorname{Tr}\left[\mathcal{H}_{T}^{2}(\lambda)\right]}$$
(8)

between Hamiltonians $\mathcal{H}_T(\lambda)$ found by IQA, at fixed l and different final times T and $T+\Delta T$. Since the operators in \mathcal{L} are orthonormal, this is the distance between the couplings vectors of the two Hamiltonians. When the annealing time T is sufficiently large, the couplings $\{h_i\}$ converge to those of the adiabatic Hamiltonian and $R_{T,\Delta T}(\lambda)$ goes to zero. Additionally, we will study the fidelity between the ground state of the adiabatic solution and the target state for different interaction ranges l.

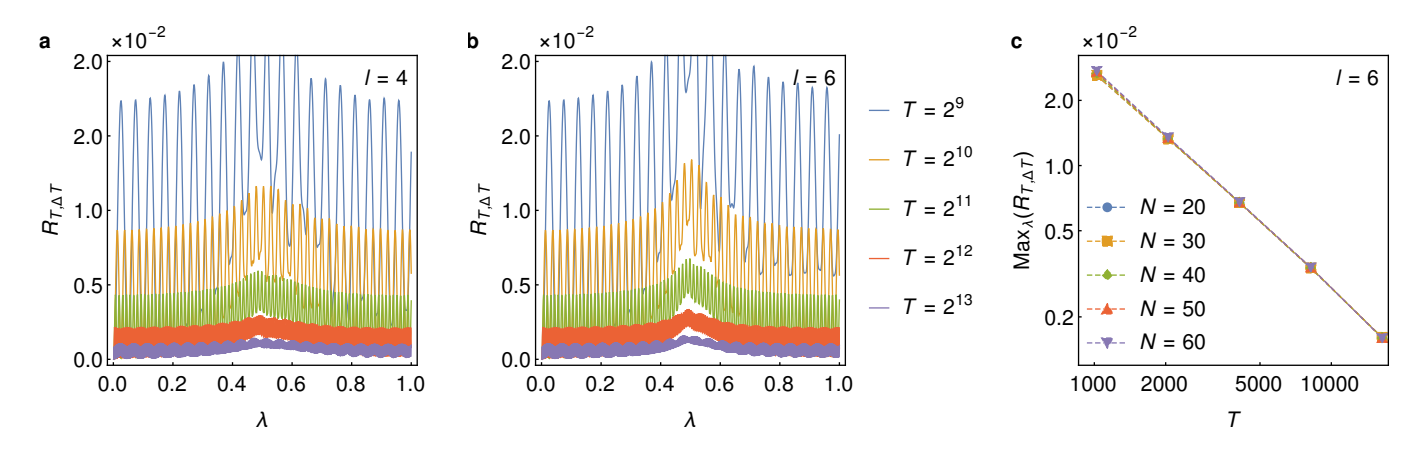


FIG. 2. Panels (a) and (b): relative distance $R_{T,\Delta T}(\lambda)$ between solutions of Eq. (6) with different annealing times T and $T + \Delta T = 2T$, for a system of N = 50. The interaction range of the Hamiltonian is l = 4 in Panel (a) and l = 6 in Panel (b). Panel (c): maximum value $\text{Max}_{\lambda}\left(R_{T,\Delta T}(\lambda)\right)$ for l = 6, as a function of the annealing time, for systems of different sizes.

In the rest of the paper, we will test the IQA in an exactly solvable case that allows us to verify its accuracy. In particular, our case study allows addressing also regimes where the correlations in the state $\psi(\lambda)$ are long-ranged, i.e., the least favorable situation for the method.

IQA with fermionic Gaussian states.— To illustrate the method, in this section, we specify our IQA procedure for the state

$$|\psi(\lambda)\rangle \equiv \prod_{k \in \mathcal{K}^+} \left(\frac{i\cos(\theta_k)}{N} \sum_{j,j'} e^{ik(j-j')} c_j^{\dagger} c_{j'}^{\dagger} + \sin(\theta_k) \right) |0\rangle,$$

where $\mathcal{K}^+ \equiv \left\{ k = \frac{(2n+1)\pi}{N}, \text{ with } n \in \{0, \dots, N/2 - 1\} \right\},$

$$\theta_k(\lambda) = \frac{1}{2}\arctan\left(\frac{\sin\left(\lambda\pi/2\right)\sin(k)}{\cos\left(\lambda\pi/2\right) + \sin\left(\lambda\pi/2\right)\cos(k)}\right),\,$$

the operator c_j^{\dagger} creates a spinless fermion on the lattice site $j \in \{1, \dots, N\}$, and $|0\rangle$ is the vacuum state. $|\psi(\lambda)\rangle$ is the ground state of the 1D Kitaev model [35]:

$$\mathcal{H}_{K}(\lambda) = J\left(\sin\left(\lambda \frac{\pi}{2}\right) \sum_{j=1}^{N} \left(c_{j}^{\dagger} c_{j+1}^{\dagger} + c_{j}^{\dagger} c_{j+1} + h. c.\right) + \cos\left(\lambda \frac{\pi}{2}\right) \sum_{j=1}^{N} \left(c_{j}^{\dagger} c_{j} - c_{j} c_{j}^{\dagger}\right),$$
(9)

where J is an energy scale, and antiperiodic boundary conditions $c_{N+1} = -c_1$ are assumed. The goal is to use the dynamics defined in Eq. (6) to determine the PH. We will compare the PH and its ground state with $|\psi(\lambda)\rangle$ to quantify the accuracy of the IQA. We choose the states $|\psi(\lambda)\rangle$ built as ground states of $\mathcal{H}_K(\lambda)$ to be sure that (at least) a 2-local parent Hamiltonian for these states exists (i. e., Eq. (9)). The annealing schedule is $\lambda(t) = t/T$, where T is the final time so that the state interpolates between $|\psi(0)\rangle$, the ground state of $\mathcal{H}_K(0)$, and $|\psi(1)\rangle$, the ground state of $\mathcal{H}_K(1)$. We perform IQA with different annealing times T to study the convergence to the adiabatic limit,

analyzing different ranges l of the interactions in $\mathcal{L}^{(l)}$, and different system sizes N. Note that $|\psi(\lambda)\rangle$ passes through a critical point at $\lambda_c = 1/2$ where the correlation length diverges. Therefore, as a consequence of the TDVP approximation, we expect IQA to work very well for paths such that $\lambda < \lambda_c$ while it may be less accurate if $\lambda \geq \lambda_c$.

The basis $\mathcal{L}^{(l)}$ of l-interacting quadratic fermions, imposing the constraints of translation and reflection invariance, is $\{\Sigma_0^Z/\sqrt{2}, \Sigma_1^\alpha, \ldots, \Sigma_l^{\alpha'}, \ldots\}$ for l < N/2, and $\mathcal{L}^{(N/2-1)} \cup \{\Sigma_{N/2}^X/\sqrt{2}, \Sigma_{N/2}^Y/\sqrt{2}\}$ for l = N/2, where $\alpha, \alpha' \in \{X,Y,Z\}$ and $\Sigma_m^X = (1/2\sqrt{N}) \sum_j (c_j^\dagger c_{j+m}^\dagger + \text{h. c.})$, $\Sigma_m^Y = (i/2\sqrt{N}) \sum_j (c_j^\dagger c_{j+m}^\dagger - \text{h. c.})$, and $\Sigma_m^Z = (1/2\sqrt{N}) \sum_j (c_j^\dagger c_{j+m}^\dagger + \text{h. c.})$. The antiperiodic boundary conditions imply $c_{N+m} \equiv -c_m$. Note that the basis $\mathcal{L}^{(N/2)}$ spans over the space of all translation-invariant quadratic fermionic Hamiltonians with antiperiodic boundary conditions. In this way, the evolution generated by $K_{ij}^{(N/2)}$ is equivalent to the non-projected evolution in Eq. (1). The generic l-local free-fermion Hamiltonian can be written as $\mathcal{H} = \sum_i h_i L_i$, where $L_i \in \mathcal{L}^{(l)}$. The commutator matrix that generates the IQA is explicitly calculated in Supplemental Material, where we also investigate the locality of the adiabatic solution of Eq. (1).

We investigate the transition to the adiabatic regime using the error $R_{T,\Delta T}(\lambda)$ in Eq. (8). In Fig. 2, we show $R_{T,\Delta T}(\lambda)$ for different annealing times T, for (a) l=4 and (b) l=6. The errors decrease by increasing the annealing time T. However, for all T's a clear peak at λ_c occurs. This peak is more pronounced for the larger range l. In Fig. 2(c), we show the maximum value of $R_{T,\Delta T}(\lambda)$, for different annealing times and system sizes. The functions $\operatorname{Max}_{\lambda}(R_{T,\Delta T}(\lambda))$ for different values of N overlap and fit to $\operatorname{Max}_{\lambda}(R_{T,\Delta T}(\lambda)) \propto 1/T$: the error is inversely proportional to the annealing time, as we expect from Eq. (3). The independence of the system size is a consequence of the fact that the expectation values corresponding to the entries of the matrix $K_{ij}^{(l)}$ converge for large N. Having determined the adiabatic regime, we fix T=

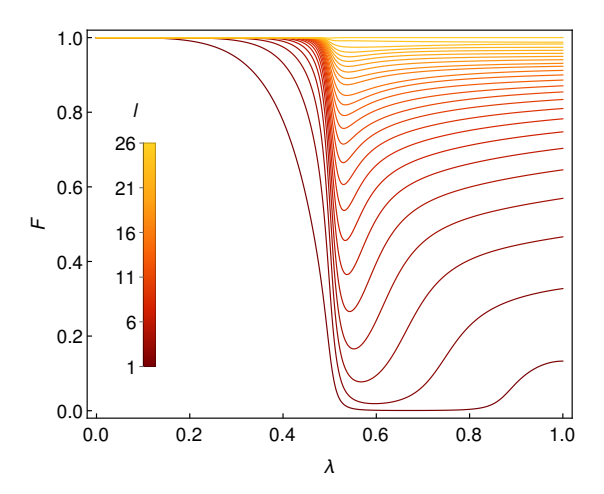


FIG. 3. Fidelity between the target state $|\psi(\lambda)\rangle$ and the ground state $|\psi^{(l)}_{GS}(\lambda)\rangle$ of the adiabatic l-local Hamiltonian $\mathcal{H}_l(\lambda)$ obtained via IQA. We consider a system of 50 sites and interactions ranges from l=1 to l=26.

16000 and investigate the properties of the PH as determined by the IQA.

In Fig. 3, we plot the fidelity $F(\lambda) = |\langle \psi_{\rm GS}^{(l)}(\lambda) | \psi(\lambda) \rangle|^2$ between the target state $|\psi(\lambda)\rangle$ and the unique ground state $|\psi_{\rm GS}^{(l)}(\lambda)\rangle$ of the adiabatic l-local Hamiltonian $\mathcal{H}_l(\lambda)$ obtained by IQA. If $\lambda < \lambda_c = 1/2$ the fidelity $F(\lambda)$ is close to 1 even for relatively small values of l. This means that our algorithm finds an optimal l-local parent Hamiltonian for the target state. The scenario changes when $\lambda > \lambda_c$. In this case, the longrange correlations of the critical point λ_c are accounted for by the IQA method only by increasing the value of l. This happens even though the Kitaev Hamiltonian is 2-local, and is reminiscent of what happens in quantum annealing at phase transitions [36].

A more quantitative analysis is obtained by looking at the fidelity as a function of l for different system sizes. If we restrict our target state to $\lambda < \lambda_c$, the fidelity is close to 1 even at small values of l, and almost independent of N, see Fig. 4(a). In Fig. 4(b), the fidelity is shown for a target state $|\psi(\lambda)\rangle$ with λ close but beyond λ_c , $\lambda = 1.1\lambda_c$. In this case, the larger l the better the fidelity, as expected.

Given a target accuracy ϵ , the l-local adiabatic Hamiltonian $\mathcal{H}_l(\lambda)$ is an optimal PH for $|\psi(\lambda)\rangle$ when the fidelity between $|\psi(\lambda)\rangle$ and the ground state $|\psi_{\mathrm{GS}}^{(l)}(\lambda)\rangle$ of $\mathcal{H}_l(\lambda)$, $F_l(\lambda) = |\langle \psi(\lambda)|\psi_{\mathrm{GS}}^{(l)}(\lambda)\rangle|^2$ is larger than $1 - \epsilon$. This condition defines a minimal interaction range l_ϵ required to adiabatically find the PH within the given accuracy ϵ , i. e., $F_l(\lambda) \geq 1 - \epsilon$ $\forall l \geq l_\epsilon$. This length l_ϵ is represented in Fig. 5 for $\epsilon = 0.005$ and different values of λ and λ . Fig. 5(a) shows that for $\lambda < \lambda_c$, l_ϵ weakly depends on the system size, while, for $\lambda > \lambda_c$, l_ϵ scales almost linearly in the system size. Fig. 5(b) shows l_ϵ versus λ for different values of λ .

Conclusions and outlook.— Quantum annealing represents one of the major examples of the computational potential of quantum many-body systems. In this work, we introduced an

annealing technique for finding the l-local Hamiltonian whose ground state is a given many-body state. We exemplified our method by reconstructing parent Hamiltonians for a non-interacting system; however, the IQA allows for the efficient reconstruction of PHs for a generic path of many-body states with finite correlation length. Moreover, our technique only relies on the knowledge of local expectation values. This last feature could be a precious ingredient for the application of IQA to the quantum marginal problem [37-42].

As a future perspective, a similar approach could allow for learning the Liouvillian dynamics of an arbitrary quantum system [43] from its stationary state. In conclusion, IQA raises a relevant challenge: the possibility to implement Eq. (1) on a quantum computer. Such an approach does not involve the TDVP, providing a PH also when $|\psi(\lambda)\rangle$ crosses a phase transition. It could be implemented, for example, by mapping the Hamiltonian $\mathcal{H}(t)$ to the state $\sigma(t) \equiv (\mathcal{H}(t) + E_0\mathbb{1})/\text{Tr}(\mathcal{H}(t) + E_0\mathbb{1})$ and implementing the unitary evolution $U_{\pi}(t)$ through the density matrix exponentiation algorithm [44, 45].

We acknowledge M. Dalmonte for his very useful suggestions and comments on the manuscript. G.P. and P.L. acknowledge financial support from the project PIR01_00011 "IBiSCo", PON 2014-2020. G.E.S., R.F. and P.L. acknowledge financial support from PNRR MUR project PE0000023-NQSTI. G.E.S. and P.L. acknowledge financial support from the project QuantERA II Programme STAQS project that has received funding from the European Union's Horizon 2020 research and innovation programme under Grant Agreement No 101017733. This work is co-funded by the European Union (ERC, RAVE, 101053159). Views and opinions expressed are however those of the author(s) only and do not necessarily reflect those of the European Union or the European Research Council. Neither the European Union nor the granting authority can be held responsible for them.

a davide.rattacaso@pd.infn.it

^[1] J. Preskill, Quantum 2, 79 (2018).

^[2] C. P. Koch, U. Boscain, T. Calarco, G. Dirr, S. Filipp, S. J. Glaser, R. Kosloff, S. Montangero, T. Schulte-Herbrüggen, D. Sugny, and F. K. Wilhelm, EPJ Quantum Technology 9, 19 (2022).

^[3] S. van Frank, M. Bonneau, J. Schmiedmayer, S. Hild, C. Gross, M. Cheneau, I. Bloch, T. Pichler, A. Negretti, T. Calarco, and S. Montangero, Scientific Reports 6, 34187 (2016).

^[4] J. Eisert, D. Hangleiter, N. Walk, I. Roth, D. Markham, R. Parekh, U. Chabaud, and E. Kashefi, Nature Reviews Physics 2, 382–390 (2020).

^[5] J. Carrasco, A. Elben, C. Kokail, B. Kraus, and P. Zoller, PRX Quantum 2, 010102 (2021).

^[6] E. Kapit and E. Mueller, Physical Review Letters 105, 215303 (2010).

^[7] M. Greiter, D. F. Schroeter, and R. Thomale, Physical Review B 89, 165125 (2014).

^[8] D. F. Schroeter, E. Kapit, R. Thomale, and M. Greiter, Physical Review Letters **99**, 097202 (2007).

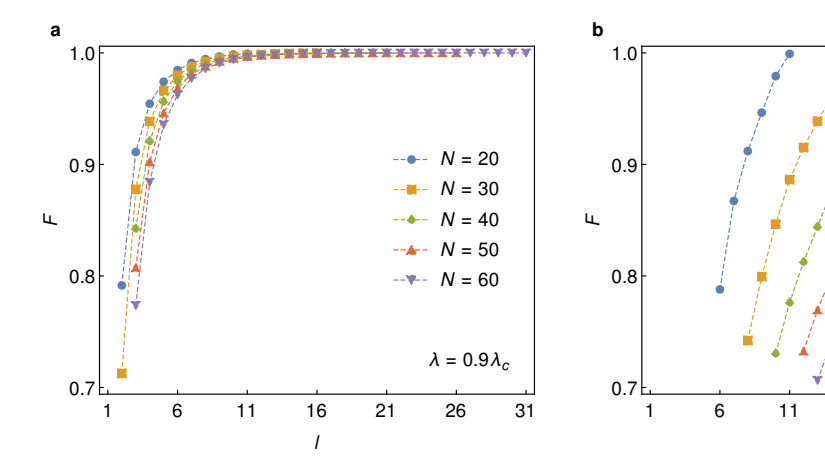


FIG. 4. Fidelity between the target state $|\psi(\lambda)\rangle$ and the ground state $|\psi_{\text{GS}}^{(l)}(\lambda)\rangle$ of the adiabatic l-local Hamiltonian $\mathcal{H}_l(\lambda)$ as a function of the interaction range l and for different system sizes N. In Panel (a) λ is just before the phase transition, i.e. at $\lambda=0.9\lambda_c$, in Panel (b) just after the phase transition, i.e. at $\lambda=1.1\lambda_c$.

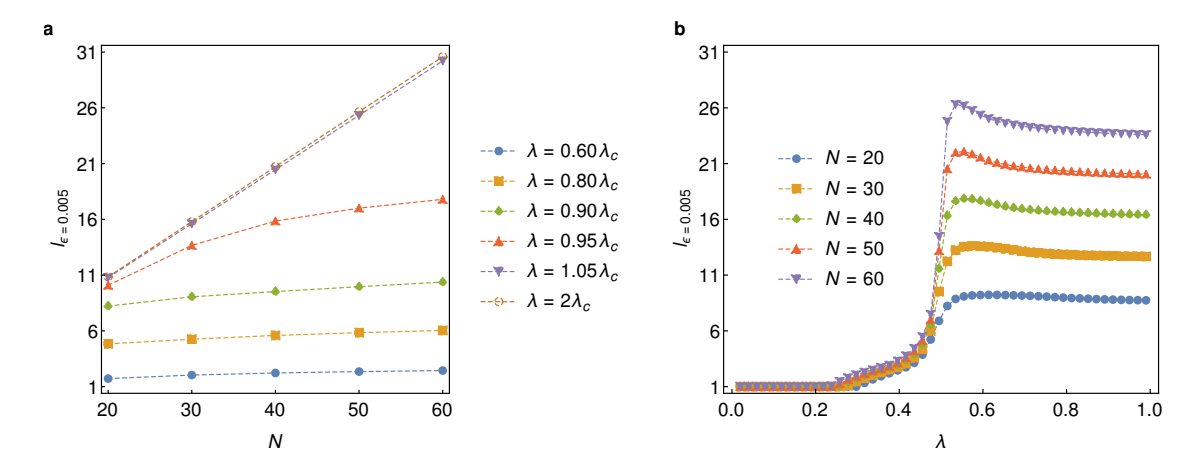


FIG. 5. Minimal interaction range l_{ϵ} required to ensure a fidelity $F \ge 1 - \epsilon$ ($\epsilon = 0.005$) between the target state and the ground state of the Hamiltonian obtained via the IQA. In Panel (a) l_{ϵ} is shown as a function of the system size and for different values of λ , in Panel (b) as a function of λ and for different system sizes.

- [9] J. Chen, Z. Ji, B. Zeng, and D. L. Zhou, Physical Review A 86, 022339 (2012).
- [10] D. Perez-Garcia, F. Verstraete, J. I. Cirac, and M. M. Wolf, Peps as unique ground states of local hamiltonians (2007), arXiv:0707.2260 [quant-ph].
- [11] C. Fernández-González, N. Schuch, M. M. Wolf, J. I. Cirac, and D. Pérez-García, Communications in Mathematical Physics 333, 299–333 (2014).
- [12] X. Turkeshi, T. Mendes-Santos, G. Giudici, and M. Dalmonte, Physical Review Letters 122, 150606 (2019).
- [13] X. Turkeshi and M. Dalmonte, SciPost Physics 8, 42 (2020).
- [14] E. Chertkov and B. K. Clark, Physical Review X 8, 031029
- [15] N. Wiebe, C. Granade, C. Ferrie, and D. G. Cory, Physical Review Letters 112, 190501 (2014).
- [16] J. Wang, S. Paesani, R. Santagati, S. Knauer, A. A. Gentile, N. Wiebe, M. Petruzzella, J. L. O'Brien, J. G. Rarity, A. Laing, and M. G. Thompson, Nature Physics 13, 551 (2017).
- [17] C. E. Granade, C. Ferrie, N. Wiebe, and D. G. Cory, New Journal

- of Physics 14, 103013 (2012).
- [18] X.-L. Qi and D. Ranard, Quantum 3, 159 (2019).
- [19] M. Greiter, V. Schnells, and R. Thomale, Physical Review B 98, 081113 (2018).

 $\lambda = 1.1 \lambda_c$

31

26

- [20] E. Bairey, I. Arad, and N. H. Lindner, Physical Review Letters 122, 020504 (2019).
- [21] S.-Y. Hou, N. Cao, S. Lu, Y. Shen, Y.-T. Poon, and B. Zeng, New Journal of Physics 22, 083088 (2020).
- [22] C. Cao, S.-Y. Hou, N. Cao, and B. Zeng, Journal of Physics: Condensed Matter 33, 064002 (2020).
- [23] A. Zubida, E. Yitzhaki, N. H. Lindner, and E. Bairey, Optimal short-time measurements for hamiltonian learning (2021), arXiv:2108.08824 [quant-ph].
- [24] D. Rattacaso, G. Passarelli, A. Mezzacapo, P. Lucignano, and R. Fazio, Physical Review A 104, 022611 (2021).
- [25] D. S. França, L. A. Markovich, V. V. Dobrovitski, A. H. Werner, and J. Borregaard, Efficient and robust estimation of many-qubit hamiltonians (2022), arXiv:2205.09567 [quant-ph].
- [26] D. Rattacaso, G. Passarelli, and P. Lucignano, Quantum 7, 905

- (2023).
- [27] T. Kadowaki and H. Nishimori, Physical Review E 58, 5355 (1998).
- [28] E. Farhi, J. Goldstone, S. Gutmann, J. Lapan, A. Lundgren, and D. Preda, Science 292, 472 (2001).
- [29] G. E. Santoro, R. Martonak, E. Tosatti, and R. Car, Science 295, 2427 (2002).
- [30] P. Hauke, H. G. Katzgraber, W. Lechner, H. Nishimori, and W. D. Oliver, Reports on Progress in Physics 83, 054401 (2020).
- [31] T. Albash and D. A. Lidar, Reviews of Modern Physics 90, 015002 (2018).
- [32] This dependence is explained by the non-Abelian Wilczek-Zee connection, which characterizes degenerate adiabatic theory [46]. Indeed, the kernel of the super-operator $-i[|\psi(\lambda(t))\rangle\langle\psi(\lambda(t))|$,] is degenerate.
- [33] J. Haegeman, J. I. Cirac, T. J. Osborne, I. Pižorn, H. Verschelde, and F. Verstraete, Physical Review Letters 107, 070601 (2011).
- [34] See Supplemental Material.
- [35] A. Y. Kitaev, Physics-Uspekhi 44, 131 (2001).
- [36] J. I. Latorre and R. Orús, Physical Review A 69, 062302 (2004).
- [37] N. Linden and W. K. Wootters, Physical Review Letters 89, 277906 (2002).
- [38] A. A. Klyachko, Journal of Physics: Conference Series 36, 72 (2006).
- [39] J. Eisert, T. Tyc, T. Rudolph, and B. C. Sanders, Communications in Mathematical Physics 280, 263 (2008).
- [40] N. Linden, S. Popescu, and W. K. Wootters, Physical Review Letters 89, 207901 (2002).
- [41] N. Wyderka, F. Huber, and O. Gühne, Physical Review A 96, 010102 (2017).
- [42] X.-D. Yu, T. Simnacher, N. Wyderka, H. C. Nguyen, and O. Gühne, Nature Communications 12, 1012 (2021).
- [43] I. L. Chuang and M. A. Nielsen, Journal of Modern Optics 44, 2455 (1997).
- [44] S. Lloyd, M. Mohseni, and P. Rebentrost, Nature Physics 10, 631 (2014).
- [45] M. Kjaergaard, M. E. Schwartz, A. Greene, G. O. Samach, A. Bengtsson, M. O'Keeffe, C. M. McNally, J. Braumüller, D. K. Kim, P. Krantz, M. Marvian, A. Melville, B. M. Niedzielski, Y. Sung, R. Winik, J. Yoder, D. Rosenberg, K. Obenland, S. Lloyd, T. P. Orlando, I. Marvian, S. Gustavsson, and W. D. Oliver, Physical Review X 12, 011005 (2022).
- [46] F. Wilczek and A. Zee, Physical Review Letters 52, 2111 (1984).
- [47] G. B. Mbeng, A. Russomanno, and G. E. Santoro, The quantum ising chain for beginners (2020), arXiv:2009.09208 [quant-ph].
- [48] P. Pfeuty, Annals of Physics 57, 79 (1970).
- [49] E. Lieb, T. Schultz, and D. Mattis, Annals of Physics 16, 407 (1961).

Supplemental Material

Time-dependent variational principle

We approximate Eq. (1) of the main text by projecting the infinitesimal Hamiltonian evolution on the closest vector of the space of local Hamiltonians. The closeness is defined through the trace distance $d(A,B) \equiv \sqrt{\text{Tr}\left[(A-B)^2\right]}$, and local Hamiltonians are spanned by the elements of $\mathcal{L}^{(l)} = \{L_i^{(l)}\}$, i. e., local operators of range l.

The resulting evolution is

$$\partial_t \mathcal{H} = \mathbb{P}(-i[|\psi(\lambda(t))\rangle\langle\psi(\lambda(t))|,\mathcal{H}]),\tag{S1}$$

where

$$\mathbb{P}(A) = \operatorname{Argmin}_{B = \sum_{i} d_{i} L_{i}^{(I)}} \operatorname{Tr} \left[(B - A)^{2} \right]$$
 (S2)

can be found imposing the nullity of derivatives as follows

$$0 = \frac{\partial}{\partial d_{i}} \operatorname{Tr} \left[(B - A)^{2} \right] \Big|_{d_{i} = d_{i}^{\operatorname{Min}}}$$

$$= \frac{\partial}{\partial d_{i}} \left[\sum_{ij} d_{i} d_{j} \operatorname{Tr} (L_{i}^{(l)} L_{j}^{(l)}) - 2 \sum_{i} d_{i} \operatorname{Tr} (L_{i}^{(l)} A) + \operatorname{Tr} (A^{2}) \right] \Big|_{d_{i} = d_{i}^{\operatorname{Min}}}$$

$$= 2 \sum_{i} d_{j}^{\operatorname{Min}} \operatorname{Tr} (L_{i}^{(l)} L_{j}^{(l)}) - 2 \operatorname{Tr} (L_{i}^{(l)} A) . \tag{S3}$$

This leads to

$$\mathbb{P}(A) = \sum_{i} d_{i}^{\text{Min}} L_{i}^{(l)} = \sum_{i} \sum_{j} \left(\text{Tr}(L_{j}^{(l)} L_{i}^{(l)}) \right)^{-1} \text{Tr}(L_{j}^{(l)} A) L_{i}^{(l)} , \qquad (S4)$$

where $(\operatorname{Tr}(L_j^{(l)}L_i^{(l)}))^{-1}$ denotes the matrix inverse. At this point, we exploit the fact that basis vectors are orthogonal $\operatorname{Tr}(L_i^{(l)}L_j^{(l)}) = Z\delta_{ij}$, up to some constant Z. The last equation becomes

$$\mathbb{P}(A) = \sum_{i} \frac{\operatorname{Tr}(AL_{i}^{(l)})}{Z} L_{i}^{(l)} . \tag{S5}$$

Replacing Eq. (S5) in Eq. (S1), we obtain

$$\partial_t \mathcal{H} = \sum_i \frac{\text{Tr}(-i[|\psi(\lambda(t))\rangle\langle\psi(\lambda(t))|, \mathcal{H}]L_i^{(l)})}{Z} L_i^{(l)}, \qquad (S6)$$

and, since $\mathcal{H}(t) = \sum_i h_i(t) L_i^{(l)}$, the corresponding equation for the Hamiltonian couplings is

$$\partial_t h_i(t) = \sum_j \frac{\text{Tr}(-i[|\psi(\lambda(t))\rangle\langle\psi(\lambda(t))|, L_j^{(l)}]L_i^{(l)})}{Z} h_j(t) = \sum_j \frac{\langle\psi(\lambda(t))| - i[L_j^{(l)}, L_i^{(l)}]|\psi(\lambda(t))\rangle}{Z} h_j(t) \ . \tag{S7}$$

We can incorporate the coefficient Z in the definition of $h_i(t)$. Therefore, the last equation is equivalent to

$$\partial_t h_i(t) = \sum_j K_{ij}^{(l)} [\psi(\lambda(t))] h_j(t) , \qquad (S8)$$

where

$$K_{ij}^{(l)}[\psi(\lambda)] \equiv \langle \psi(\lambda)| - i[L_i^{(l)}, L_i^{(l)}]|\psi(\lambda)\rangle \tag{S9}$$

is the commutator matrix.

Basis of quadratic fermionic Hamiltonians

We define the basis $\mathcal{L}^{(l)}$ of a space of translation and reflection invariant interactions of range l as follows:

$$\mathcal{L}^{(l < N/2)} \equiv \{ \Sigma_0^Z / \sqrt{2}, \Sigma_1^X, \Sigma_1^Y, \Sigma_1^Z, \dots, \Sigma_l^X, \Sigma_l^Y, \Sigma_l^Z \},$$

and

$$\mathcal{L}^{(N/2)} \equiv \mathcal{L}^{(N/2-1)} \cup \{ \sum_{N/2}^{X} / \sqrt{2}, \sum_{N/2}^{Y} / \sqrt{2} \},$$

where

$$\begin{split} \Sigma_{m}^{X} &= \frac{1}{2\sqrt{N}} \sum_{j=1}^{N} \left(c_{j}^{\dagger} c_{j+m}^{\dagger} - c_{j} c_{j+m} \right) \\ \Sigma_{m}^{Y} &= \frac{i}{2\sqrt{N}} \sum_{j=1}^{N} \left(c_{n}^{\dagger} c_{j+m}^{\dagger} + c_{j} c_{j+m} \right) \\ \Sigma_{m}^{Z} &= \frac{1}{2\sqrt{N}} \sum_{i=1}^{N} \left(c_{j}^{\dagger} c_{j+m} - c_{j} c_{j+m}^{\dagger} \right) \end{split} \tag{S10}$$

with c_j^{\dagger} and c_j fermionic creation and annihilation operators at position j on the lattice, and antiperiodic boundary conditions $c_{N+m} \equiv -c_m$.

The operators in $\mathcal{L}^{(l)}$ allow for a common block-diagonal representation [47]. As a first step in this direction, we introduce the fermionic operators c_k in the reciprocal space:

$$c_k = \frac{e^{-i\pi/4}}{\sqrt{N}} \sum_{j=1}^{N} e^{-ikj} c_j .$$

The antiperiodic boundary conditions $c_{N+m} = -c_m$ imply that $\sum_{k \in \mathcal{K}} e^{ik(N+m)} c_k = -\sum_{k \in \mathcal{K}} e^{ikm} c_k$, that is

$$k \in \mathcal{K} \equiv \left\{ k = \frac{(2n+1)\pi}{N}, \text{ with } n \in \{0, \dots, N-1\} \right\}.$$

Now the operators in $\mathcal{L}^{(l)}$ can be written as :

$$\begin{split} &\Sigma_{m}^{X} = -\frac{i}{2\sqrt{N}} \sum_{k \in \mathcal{K}} (e^{imk} c_{k}^{\dagger} c_{-k}^{\dagger} - e^{-imk} c_{-k} c_{k}) = \frac{1}{\sqrt{N}} \sum_{k \in \mathcal{K}} \sin(mk) (c_{k}^{\dagger} c_{-k}^{\dagger} + c_{-k} c_{k}) \\ &\Sigma_{m}^{Y} = \frac{1}{2\sqrt{N}} \sum_{k \in \mathcal{K}} (e^{imk} c_{k}^{\dagger} c_{-k}^{\dagger} + e^{-imk} c_{-k} c_{k}) = \frac{i}{\sqrt{N}} \sum_{k \in \mathcal{K}} \sin(mk) (c_{k}^{\dagger} c_{-k}^{\dagger} - c_{-k} c_{k}) \\ &\Sigma_{m}^{Z} = \frac{1}{2\sqrt{N}} \sum_{k \in \mathcal{K}} e^{imk} (c_{k}^{\dagger} c_{k} + c_{-k}^{\dagger} c_{-k} - \mathbb{1}) = \frac{1}{\sqrt{N}} \sum_{k \in \mathcal{K}} \cos(mk) (c_{k}^{\dagger} c_{k} + c_{-k}^{\dagger} c_{-k} - \mathbb{1}) \;, \end{split} \tag{S11}$$

where we have taken into account the relationships

$$\begin{split} c_k^{\dagger} c_k + c_{-k}^{\dagger} c_{-k} &= c_{-k}^{\dagger} c_{-k} + c_k^{\dagger} c_k \\ c_k^{\dagger} c_{-k}^{\dagger} &= -c_{-k}^{\dagger} c_k^{\dagger} \\ c_k c_{-k} &= -c_{-k} c_k \; . \end{split}$$

Finally, let us define the pseudospin operators $\tilde{\sigma}_k^x = c_k^\dagger c_{-k}^\dagger + c_{-k} c_k$, $\tilde{\sigma}_k^y = -i(c_k^\dagger c_{-k}^\dagger - c_{-k} c_k)$, and $\tilde{\sigma}_k^z = c_k^\dagger c_k + c_{-k}^\dagger c_{-k} - 1$. These operators form a representation of the spin algebra on the lattice of momenta, i. e., $\{\tilde{\sigma}_k^\mu, \tilde{\sigma}_l^\nu\} = 21\delta_{kl}\delta_{\mu\nu}$ and $[\tilde{\sigma}_k^\mu, \tilde{\sigma}_l^\nu] = 2i\varepsilon_{\mu\nu\gamma}\delta_{kl}\tilde{\sigma}_k^\gamma$, where $\varepsilon_{\mu\nu\gamma}$ is the Levi-Civita symbol. In terms of pseudospins, the operators in $\mathcal{L}^{(l)}$ read

$$\begin{split} \Sigma_{m}^{X} &= \frac{2}{\sqrt{N}} \sum_{k \in \mathcal{K}^{+}} \sin(mk) \tilde{\sigma}_{k}^{X} \\ \Sigma_{m}^{Y} &= \frac{2}{\sqrt{N}} \sum_{k \in \mathcal{K}^{+}} \sin(mk) \tilde{\sigma}_{k}^{Y} \\ \Sigma_{m}^{Z} &= \frac{2}{\sqrt{N}} \sum_{k \in \mathcal{K}^{+}} \cos(mk) \tilde{\sigma}_{k}^{Z}, \end{split} \tag{S12}$$

where $\mathcal{K}^+ \equiv \{ k = (2n+1)\pi/N, \text{ with } n \in \{0, ..., N/2 - 1\} \}.$

Now, we show that the operators in $\mathcal{L}^{(N/2)}$ are orthogonal and that they have the same norm. First, let us remark that $\text{Tr}(\tilde{\sigma}_k^{\mu}\tilde{\sigma}_{k'}^{\nu}) = \text{Tr}(\{\tilde{\sigma}_k^{\mu},\tilde{\sigma}_{k'}^{\nu}\})/2 = \text{Tr}(\mathbb{1})\delta_{kk'}\delta_{\mu\nu}$. It follows that the scalar products of the operators Σ_m^{μ} are

$$\operatorname{Tr}\left(\Sigma_{m}^{\mu}\Sigma_{l}^{\nu}\right) = \frac{4}{N} \sum_{k} \sum_{k'} \operatorname{Tr}(\tilde{\sigma}_{k}^{\mu} \tilde{\sigma}_{k'}^{\nu}) f^{\mu}(km) f^{\nu}(k'l) = \frac{4}{N} \delta_{\mu\nu} \operatorname{Tr}(\mathbb{1}) \sum_{k} f^{\mu}(km) f^{\mu}(kl), \tag{S13}$$

where $f^{\mu}(x) \equiv (\sin(x), \sin(x), \cos(x))$. Considering the orthogonality of the Fourier basis, the latter equation becomes

$$\operatorname{Tr}\left(\Sigma_{m}^{\mu}\Sigma_{l}^{\nu}\right) = \delta_{\mu\nu}\delta_{ml}\frac{1}{2}\operatorname{Tr}(\mathbb{1}) \qquad \text{for} \quad 0 < m < N/2$$

$$\operatorname{Tr}\left(\Sigma_{m}^{\mu}\Sigma_{l}^{\nu}\right) = \delta_{\mu\nu}\delta_{ml}\operatorname{Tr}(\mathbb{1}) \qquad \text{for} \quad m \in \{0, N/2\} \ . \tag{S14}$$

Therefore,

$$\mathcal{L}^{(N/2)} \equiv \{ \Sigma_0^Z / \sqrt{2}, \Sigma_1^X, \Sigma_1^Y, \Sigma_1^Z, \dots, \Sigma_{N/2-1}^X, \Sigma_{N/2-1}^Y, \Sigma_{N/2-1}^Z, \Sigma_{N/2}^X / \sqrt{2}, \Sigma_{N/2}^Y / \sqrt{2} \},$$
 (S15)

is a set of 3N/2 orthogonal vectors with the same norm.

Hamiltonian diagonalization and commutator matrix

Here we calculate commutator matrix $K_{ij}^{(l)}(\lambda)$, i.e., more explicitly $K_{\{n,\nu\}\{m,\mu\}}^{(l)}(\lambda) \equiv \langle \psi(\lambda)| - i[\Sigma_m^{\mu}, \Sigma_n^{\nu}]|\psi(\lambda)\rangle$. These are the commutators expectation values of the the operators in $\mathcal{L}^{(l)}$ for the ground states $|\psi(\lambda)\rangle$ of

$$H_{K}(\lambda) = \sin\left(\lambda \frac{\pi}{2}\right) \sum_{j=1}^{N} \left(c_{j}^{\dagger} c_{j+1}^{\dagger} + c_{j}^{\dagger} c_{j+1}^{\dagger} + \text{h.c.}\right) + \cos\left(\lambda \frac{\pi}{2}\right) \sum_{j=1}^{N} \left(c_{j}^{\dagger} c_{j}^{\dagger} - c_{j}^{\dagger} c_{j}^{\dagger}\right). \tag{S16}$$

Exploiting Eqs. (S12), this Hamiltonian can be written in pseudospin form as

$$H_{K}(\lambda) = -\sum_{k \in \mathcal{K}^{+}} \epsilon_{k} \left(v_{k}^{x} \tilde{\sigma}_{k}^{x} + v_{k}^{y} \tilde{\sigma}_{k}^{z} \right), \tag{S17}$$

where

$$\epsilon_{k} = \sqrt{1 + 2\sin(\lambda \pi/2)\cos(\lambda \pi/2)\cos(k)}$$

$$v_{k}^{x} = -\sin(\lambda \pi/2)\sin(k)/\epsilon_{k}$$

$$v_{k}^{z} = -(\cos(\lambda \pi/2) + \sin(\lambda \pi/2)\cos(k))/\epsilon_{k}.$$
(S18)

The density matrix of the ground states of $H^{K}(\lambda)$ is

$$\rho(\lambda) \equiv \bigotimes_{k \in \mathcal{K}^+} \left(v_k^x \tilde{\sigma}_k^x + v_k^z \tilde{\sigma}_k^z + \mathbb{1} \right) / 2. \tag{S19}$$

We will exploit this density matrix representation of the state to evaluate the commutator matrix. The corresponding state $|\psi(\lambda)\rangle$ is the +1 eigenvector of $\rho(\lambda)$:

$$|\psi(\lambda)\rangle \equiv \prod_{k \in \mathcal{K}^+} \left(\cos(\theta_k(\lambda)) \tilde{\sigma}_k^x + \sin(\theta_k(\lambda)) \mathbb{1} \right) |\downarrow_k\rangle, \tag{S20}$$

where

$$\theta_k(\lambda) = \frac{1}{2}\arctan\left(\frac{\sin(\lambda\pi/2)\sin(k)}{\cos(\lambda\pi/2) + \sin(\lambda\pi/2)\cos(k)}\right). \tag{S21}$$

In the standard fermionic formalism, this reads:

$$|\psi(\lambda)\rangle \equiv \prod_{k \in \mathcal{K}^{+}} \left(\cos(\theta_{k}(\lambda)) c_{k}^{\dagger} c_{-k}^{\dagger} + \sin(\theta_{k}(\lambda)) \mathbb{1} \right) |0\rangle, \tag{S22}$$

where $|0\rangle$ is the vacuum state. Thanks to a Fourier transform, we can represent the ground states in position space as

$$|\psi(\lambda)\rangle \equiv \prod_{k \in \mathcal{K}^+} \left(\frac{i}{N} \cos(\theta_k) \sum_{j,j'} e^{ik(j-j')} c_j^{\dagger} c_{j'}^{\dagger} + \sin(\theta_k) \right) |0\rangle . \tag{S23}$$

The commutator matrix is related to the pseudospin commutator matrix $K'_{\{k,\alpha\}\{k',\alpha'\}}(\lambda) \equiv \langle \psi(\lambda)| - i[\tilde{\sigma}^{\alpha'}_{k'}, \tilde{\sigma}^{\alpha}_{k}]|\psi(\lambda)\rangle$ as follows:

$$K_{\{n,\nu\}\{m,\mu\}}^{(l)} = \langle \psi(\lambda)| - i[\Sigma_m^{\mu}, \Sigma_n^{\nu}] | \psi(\lambda) \rangle = \sum_{k,k'}^{\mathcal{H}^+} \sum_{\alpha,\alpha'}^{X,Y,Z} \mathcal{F}_{\{n,\nu\}\{k,\alpha\}}^{(l)} \mathcal{F}_{\{m,\mu\}\{k',\alpha'\}}^{(l)} K_{\{k,\alpha\}\{k',\alpha'\}}',$$
 (S24)

where $\mathcal{F}^{(l)}_{\{n,\nu\}\{k,\alpha\}}$ is a matrix Fourier transform. In particular, for l < N/2 we have:

$$\mathcal{F}^{(l)} = \frac{1}{\sqrt{N}} \begin{pmatrix} 0 & 0 & 1/\sqrt{2} & 0 & 0 & 1/\sqrt{2} & \dots \\ \sin(1k_1) & 0 & 0 & \sin(1k_2) & 0 & 0 & \dots \\ 0 & \sin(1k_1) & 0 & 0 & \sin(1k_2) & 0 & \dots \\ 0 & 0 & \cos(1k_1) & 0 & 0 & \cos(1k_2) & \dots \\ \dots & \dots & \dots & \dots & \dots & \dots \\ \sin(lk_1) & 0 & 0 & \sin(lk_2) & 0 & 0 & \dots \\ 0 & \sin(lk_1) & 0 & 0 & \sin(lk_2) & 0 & \dots \\ 0 & 0 & \cos(lk_1) & 0 & 0 & \cos(lk_2) & \dots \end{pmatrix}, \tag{S25}$$

and for l = N/2:

$$\mathcal{F}^{(N/2)} = \frac{1}{\sqrt{N}} \begin{pmatrix} 0 & 0 & 1/\sqrt{2} & 0 & 0 & 1/\sqrt{2} & \dots \\ \sin(1k_1) & 0 & 0 & \sin(1k_2) & 0 & 0 & \dots \\ 0 & \sin(1k_1) & 0 & 0 & \sin(1k_2) & 0 & \dots \\ 0 & 0 & \cos(1k_1) & 0 & 0 & \cos(1k_2) & \dots \\ \vdots & \vdots \\ \cos(\frac{N}{2} - 1)k_1) & 0 & 0 & \sin(\frac{N}{2} - 1)k_2) & 0 & 0 & \dots \\ 0 & \sin(\frac{N}{2} - 1)k_1) & 0 & 0 & \sin(\frac{N}{2} k_2) & 0 & \dots \\ 0 & 0 & \cos((\frac{N}{2} - 1)k_1) & 0 & 0 & \cos((\frac{N}{2} - 1)k_2) & \dots \\ \sin(Nk_1/2)/\sqrt{2} & 0 & 0 & \sin(Nk_2/2)/\sqrt{2} & 0 & 0 & \dots \\ 0 & \sin(Nk_1/2)/\sqrt{2} & 0 & 0 & \sin(Nk_2/2)/\sqrt{2} & 0 & \dots \end{pmatrix}$$

$$(S26)$$

The last step consists in calculating the elements of the matrix $K'(\lambda)$. Thanks to the simple commutation rules between pseudospins, this is a block-diagonal matrix:

$$K'(\lambda) = \begin{pmatrix} K_{k_1}(\lambda) & 0 & \dots \\ 0 & K_{k_2}(\lambda) & \dots \\ \dots & \dots & \dots \end{pmatrix}, \tag{S27}$$

where the blocks are labelled by the elements of \mathcal{K}^+ . Exploiting Eq. (S19), we obtain the explicit form of the submatrices:

$$K_k(\lambda) = \begin{pmatrix} 0 & v_k^z(\lambda) & 0 \\ -v_k^z(\lambda) & 0 & v_k^x(\lambda) \\ 0 & -v_k^x(\lambda) & 0 \end{pmatrix}.$$
 (S28)

Now, the commutator matrix can be easily calculated through the Fourier transform of $K'(\lambda)$:

$$K^{(l)}(\lambda) = (\mathcal{F}^{(l)})(K'(\lambda))(\mathcal{F}^{(l)})^{\mathrm{T}}.$$
 (S29)

Non-projected IQA with fermion Gaussian states

Gaussian states allow us to study the IQA for large system sizes without the TDVP, allowing us to test our claim that the dynamics of Eq. (1) generates l-local PHs for states with finite correlation length. We refer to the adiabatic solution to Eq. (1)

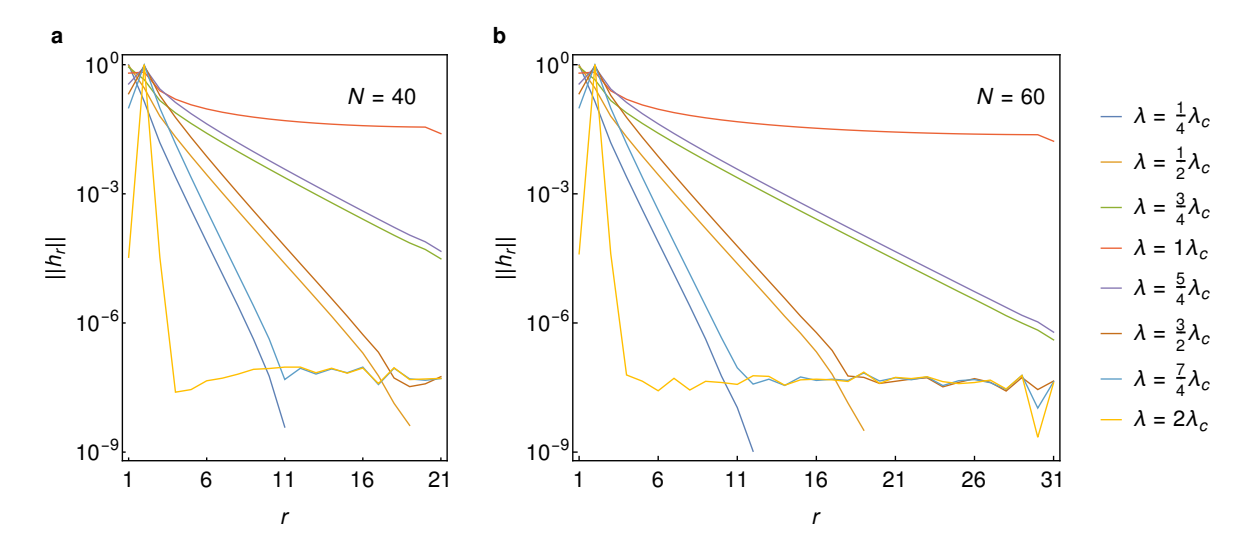


FIG. S1. Norm of the non-projected adiabatic Hamiltonian couplings of different ranges r. Panel (a): for N = 40 sites, Panel (b): for N = 50 sites

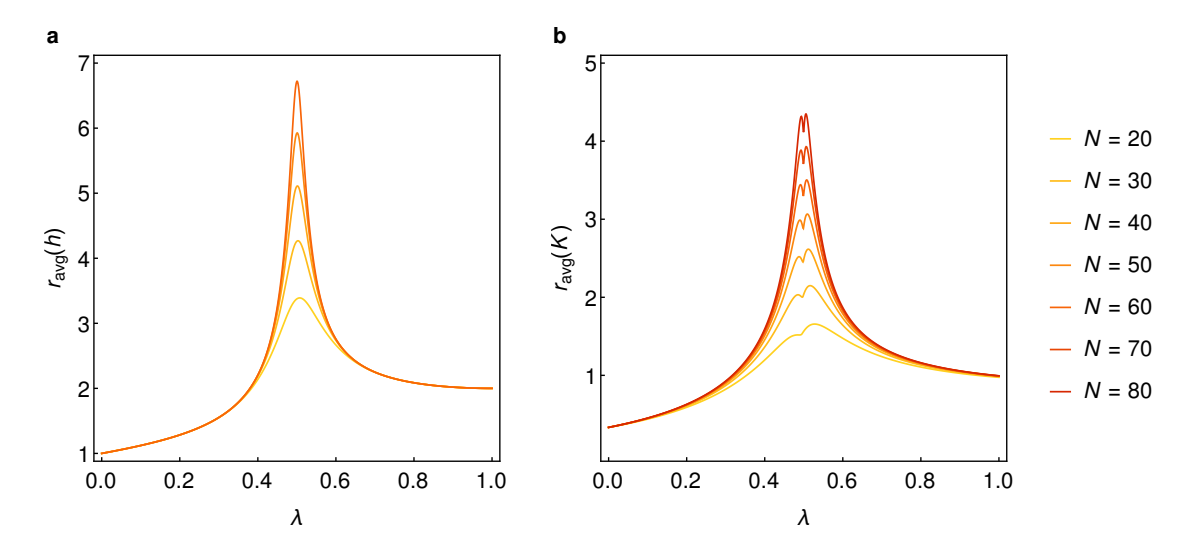


FIG. S2. Panel(a): effective interaction range of the non-projected adiabatic Hamiltonian. Panel (b): correlation range of $K_{ij}^{(N/2)}$.

as *non-projected* adiabatic Hamiltonian. The non-projected adiabatic Hamiltonian corresponds to equation Eq. (6) for l = N/2. Here, we study the link between the (effective) interaction range of this Hamiltonian and the correlation length of $|\psi(\lambda)\rangle$. In Fig. S1, we plot the total norm

$$||h_r|| = \sqrt{\sum_{i: \text{range}(L_i^l) = r} h_i^2}$$

of the couplings of range r of this Hamiltonian at different values of λ , for a system of 40 (a) and 60 (b) sites. We observe that this norm exponentially decays with r for $\lambda \neq \lambda_c = 1/2$ with a decay rate that does not depend on the system size. We can confirm that Eq. (1) generates a local PH, but only for non-critical states.

We can define an effective interaction range as

$$r_{\text{avg}}(h) \equiv \frac{\sum_r r \|h_r\|}{\sum_r \|h_r\|}.$$

This range is represented in Fig. S2(a). We can see that, for sufficiently large N, it does not depend on the system size for non-critical states. However, it diverges linearly with N at $\lambda = \lambda_c$. This scaling is reminiscent of the correlation length of $|\psi(\lambda)\rangle$.

To understand how the scaling behavior originated in the equation of motion, we look at the commutator matrix $K_{ii}^{(N/2)}$. We define a correlation range for this matrix

$$r_{\text{avg}}(K) \equiv \frac{\sum_{i,j} |i-j| |K_{ij}|}{\sum_{i,j} |K_{ij}|},$$

which measures the decay of non-diagonal elements. It is depicted in Fig. S2(b), and follows the same scaling behavior as the previously analyzed functions. We can conclude that, when the correlation length of states is finite, the non-projected dynamics weakly couples the local and non-local operators and the Hamiltonian does not delocalize.

Relationship with spin systems

Here we show that, thanks to the Jordan-Wigner transformations [47], all the operators in $\mathcal{L}^{(l)}$ are equivalent to a set of spin strings spanning over a space of Hamiltonians that encloses several important physical models, such as the Ising model in transverse field [48] and the XY model [49]. As a consequence, our results about Gaussian states can be extended to a large class of spins systems.

We consider the operators in $S = \{S_0^Z, S_1^X, S_1^Y, S_1^Z, \dots, S_{N/2-1}^X, S_{N/2-1}^Y, S_{N/2-1}^Z, S_{N/2}^X, S_{N/2}^Y\}$ acting on a system of N spins,

$$S_{0}^{Z} = -\frac{1}{2\sqrt{N}} \sum_{j}^{N} \sigma_{j}^{z}$$

$$S_{m}^{X} = \frac{1}{4\sqrt{N}} \sum_{j}^{N} \left(\sigma_{j}^{x} \sigma_{j+1}^{z} \dots \sigma_{j+m-1}^{z} \sigma_{j+m}^{x} - \sigma_{j}^{y} \sigma_{j+1}^{z} \dots \sigma_{j+m-1}^{z} \sigma_{j+m}^{y} \right)$$

$$S_{m}^{Y} = \frac{1}{4\sqrt{N}} \sum_{j}^{N} \left(\sigma_{j}^{x} \sigma_{j+1}^{z} \dots \sigma_{j+m-1}^{z} \sigma_{j+m}^{y} + \sigma_{j}^{y} \sigma_{j+1}^{z} \dots \sigma_{j+m-1}^{z} \sigma_{j+m}^{x} \right)$$

$$S_{m}^{Z} = \frac{1}{4\sqrt{N}} \sum_{j}^{N} \left(\sigma_{j}^{x} \sigma_{j+1}^{z} \dots \sigma_{j+m-1}^{z} \sigma_{j+m}^{x} + \sigma_{j}^{y} \sigma_{j+1}^{z} \dots \sigma_{j+m-1}^{z} \sigma_{j+m}^{y} \right), \tag{S30}$$

where N is even and the boundary conditions are periodic: $\sigma_{j+N}^{\mu} = \sigma_{j}^{\mu}$. Let us consider the parity operator $P \equiv \prod_{n} \sigma_{n,z}$. P commutes with each element of \mathcal{L} , so we can divide the whole Hilbert space in two parity sectors and write the S_n^{μ} in a block-diagonal form:

$$S_n^{\mu} = \begin{pmatrix} S_{n,0}^{\mu} & 0\\ 0 & S_{n,1}^{\mu} \end{pmatrix},\tag{S31}$$

where the subscript $p \in \{0, 1\}$ in $S_{n,p}^{\mu}$ is referred to the parity of the Hilbert subspace on which the operator acts (0 even, 1 odd). We define the Jordan-Wigner transformations

$$K_{j} = \prod_{j'=1}^{j-1} (\mathbb{1} - 2c_{j'}^{\dagger} c_{j'})$$

$$\sigma_{j}^{z} = (\mathbb{1} - 2c_{j}^{\dagger} c_{j})$$

$$\sigma_{j}^{x} = K_{j} (c_{j}^{\dagger} + c_{j})$$

$$\sigma_{j}^{y} = i K_{j} (c_{j}^{\dagger} - c_{j}), \qquad (S32)$$

where the c_j^{\dagger} 's and the c_j 's are fermionic creation and annihilation operators in position space. After some algebra, the action of the basis elements in the even parity sector, that contains the ground states of the Hamiltonians spanned by S, can be written as:

$$S_{0,0}^{Z} = \Sigma_{0}^{Z}$$

$$S_{m,0}^{X} = \Sigma_{m}^{X}$$

$$S_{m,0}^{Y} = \Sigma_{m}^{Y}$$

$$S_{m,0}^{Z} = \Sigma_{m}^{Z},$$
(S33)

with antiperiodic boundary conditions $c_{N+m} \equiv -c_m$ and $1 \le m \le N/2$.